

# We are IntechOpen, the world's leading publisher of Open Access books Built by scientists, for scientists

6,900

Open access books available

185,000

International authors and editors

200M

Downloads

Our authors are among the

154

Countries delivered to

TOP 1%

most cited scientists

12.2%

Contributors from top 500 universities



WEB OF SCIENCE™

Selection of our books indexed in the Book Citation Index  
in Web of Science™ Core Collection (BKCI)

Interested in publishing with us?  
Contact [book.department@intechopen.com](mailto:book.department@intechopen.com)

Numbers displayed above are based on latest data collected.  
For more information visit [www.intechopen.com](http://www.intechopen.com)



---

# Design of Robust Digital Pole Placer for Car Active Suspension with Input Constraint

---

Hisham M. Soliman, Rashid Al-Abri and  
Mohammed Albadi

Additional information is available at the end of the chapter

<http://dx.doi.org/10.5772/intechopen.70587>

---

## Abstract

This chapter deals with the problem of state feedback control for an active quarter-car suspension system with control input constraint. The dynamics of the suspension system is first formed in terms of the control objectives: ride comfort, suspension deflection, and maximum actuator control force. The control task is formulated as robustly placing the closed poles in a desired region against different passenger load. Since digital computers are widely used in the vehicle industry, a new saturated controller design method is presented for regional pole-placement of uncertain discrete time systems. The constraint of control input saturation is considered in the design phase. The desired dynamic performance for uncertain discrete-time systems is represented by the settling time and damping ratio. A sufficient condition is derived to place the poles in a desired region. The design is formulated in terms of linear matrix inequality optimization. The effectiveness of the proposed design is illustrated by applying it to a quarter-car active suspension system. Different road tests for the proposed controller are carried out: step and bump disturbances. The proposed design achieves the desired oscillation damping due to road disturbances in addition to passenger comfort. The results are compared with the passive suspension system.

**Keywords:** constrained control, regional pole placement, linear matrix inequality (LMI) optimization, discrete-time systems, vehicle active suspension

---

## 1. Introduction

The design of a car suspension system is of paramount importance for improving the ride comfort, maintaining vehicle maneuverability, and retaining the safety of passengers [1]. Vehicle suspension systems include wishbone, spring, and shock absorber (e.g., damper) to transmit and mitigate forces between the car body and the road. This contributes to the passenger

---

comfort and the ride. However, the widely used passive suspension systems which use springs and dampers with fixed parameters (stiffness and damper coefficients) do not achieve satisfactory suspension performance under wider driving maneuvers. This problem is alleviated by the recent developments of semi-active suspension and active suspension [2].

Semi-active suspensions use the springs and dampers whose parameters (e.g., stiffness and damper coefficients) are adjusted corresponding to different vehicle driving scenarios [3]. These varying parameters provide considerable improvements over passive suspension systems. However, special springs and/or dampers (e.g., a magneto rheological fluid, MR, damper) are used in this case, and the construction and tuning of such components are not easy. Moreover, using such elements can lead to potential difficulties, for example, MR dampers exhibit hysteresis dynamics, which are highly nonlinear and difficult to model.

Active suspension has attracted extensive research because in this framework an extra actuator is placed between the car body and the wheel-axle. It is installed in parallel to other suspension mechanisms (e.g., damper and spring [4]). So, this actuator can be controlled to dissipate energy from the road disturbances and thus reduces the impact on the displacement of vehicles. It is well known that active suspension requires high energy demand and cost. Therefore, active suspensions have not been widely used in commercial vehicles. However, it is expected that active suspension techniques will be adopted by the industry due to its potentials to improve the suspension performance.

Extensive research work on active suspension has been carried out in the past few decades [5, 6]. A crucial issue in the active suspension system designs is the control strategies, which should make the actuators pull down or push up the suspension motions and also achieve other suspension requirements. A model-reaching adaptive control is presented in [7] to achieve the ideal isolation of a skyhook target; the vehicle maintains a stable posture. An LPV gain-scheduling controller is proposed in [8] for a quarter-vehicle active suspension system. To manage the trade-off between the conflicting performances, the  $H^\infty$  control method can manage the trade-off and obtain a compromise performance [9, 10]. An  $H^\infty$  control is designed for active suspension systems that are subject to actuator time delay which is given in [11]. Sampled-data  $H^\infty$  control of uncertain active suspension systems via fuzzy control is presented in [12]. Adaptive sliding-mode control for active suspensions using fuzzy approach is shown in [13]. In [14], a linear-quadratic-Gaussian (LQG) control is used to obtain a trade-off between the conflicting suspension requirements.

Many physical systems are inherently nonlinear and subject to variation in the operating point. To overcome such difficulties, the system to be controlled is represented by an uncertain linear time-invariant model. The uncertainty can be cast into either polytopic or norm-bounded form. The powerful, robust control techniques of linear systems can then be applied [15]. The poles of systems without uncertainty can be placed in desired locations so as to achieve good dynamic behavior in terms of settling time and damping ratio [16]. However, for systems with uncertainties, the closed-loop poles can be assigned to a domain (D) or region, rather than specific locations [17]. This is termed D-stability or regional pole placement by using robust controllers against system uncertainty. Regional pole placement for continuous-time systems with polytopic uncertainty using state feedback is presented in [18], while output feedback is

presented in [19]. Regional pole placement with guaranteed-cost control of active suspension system of a quarter-car model is given in [20].

In many practical control problems, the actuator has limited output, called saturated (or constrained) control [21]. Combining robust pole placement with saturated control is termed multi-objective control. When the actuator saturation is not considered in the design phase, the performance of the designed control system seriously deteriorates. A state-feedback control achieving guaranteed-cost regional pole placement with the control limits, i.e., the actuator force must not exceed a certain limit, is presented in [22] for continuous-time case.

This chapter is concerned with the digital state-feedback controller design problem for active quarter-car suspension systems. The main contributions of this chapter can be summarized as follows: (1) formulate multi-object control constraints in LMIs via state-feedback control approach for the suspension vehicle system and (2) construct a simple new-type state-feedback controller. The proposed design achieves four constraints: (1) damps effectively the car oscillations due to disturbance of road irregularities, (2) robustness against different car loads, (3) no control limits violation, and (4) optimal passenger comfort against road roughness. It is expected that the proposed research pave the way for implementing the theoretical findings into vehicle suspension systems.

**Notations:** Capital and small letters denote matrices and vectors, respectively.  $I$  and  $0$  denote the identity matrix and zero matrix, respectively.  $W'$  and  $W^{-1}$  denote the transpose and the inverse of any square matrix  $W$ , respectively.  $W > 0$  ( $W < 0$ ) denotes a symmetric positive (negative)-definite matrix  $W$ . The symbol  $\bullet$  is as an ellipsis for terms in matrix expressions that are induced by symmetry. For example,

$$\begin{bmatrix} L + (W + N + W' + N') & N \\ N' & M \end{bmatrix} = \begin{bmatrix} L + (W + N + \bullet) & N \\ \bullet & M \end{bmatrix} \quad (1)$$

**Facts:** the following facts [15] are used in the sequel:

Fact 1 (congruence transformation):

The definiteness of a matrix  $W$  does not change under the congruence transformation  $H'WH$ .

Fact 2:

For any real matrices  $W_1$ ,  $W_2$  and  $\Delta_k$  with appropriate dimensions and  $\Delta_k' \Delta_k \leq I$ ,  $\leftrightarrow \|\Delta_k\| \leq 1$ , it follows that

$$W_1 \Delta_k W_2 + \dots W_2' \Delta_k' W_1' \leq \varepsilon^{-1} W_1 W_1' + \varepsilon W_2' W_2, \dots \varepsilon > 0 \quad (2)$$

where  $\Delta_k$  represents system uncertainty at discrete time  $k$ . The use of this lemma is to eliminate the uncertainty.

Fact 3 (Schur complement):

This fact is useful in transforming a nonlinear matrix inequality into a linear one.

For constant matrices  $W_1$ ,  $W_2$ , and  $W_3$ , where  $W_1' = W_1$  and  $0 < W_2 = W_2'$ , it follows that

$$W_1 + W_3' W_2^{-1} W_3 < 0 \leftrightarrow \begin{bmatrix} W_1 & W_3' \\ W_3 & -W_2 \end{bmatrix} < 0 \quad (3)$$

## 2. Problem formulation

The quarter-vehicle suspension model is shown in **Figure 1** [9].

The dynamics of the quarter-car model can be described by the state equation as follows [9]:

$$\dot{x} = Ax + Bu + D_w w, x(0) = x_0 \quad (4)$$

where

$$A = \begin{bmatrix} 0 & 1 & 0 & -1 \\ \frac{-k_s}{M_s} & \frac{-c_s}{M_s} & 0 & \frac{c_s}{M_s} \\ 0 & 0 & 0 & 1 \\ \frac{k_s}{m} & \frac{c_s}{m} & \frac{-k_t}{m} & \frac{-c_s}{m} \end{bmatrix}, D_w = \begin{bmatrix} 0 \\ 0 \\ -1 \\ 0 \end{bmatrix}, B = \begin{bmatrix} 0 \\ \frac{u_s}{M_s} \\ 0 \\ \frac{-u_s}{m} \end{bmatrix} \quad (5)$$

where  $k_s$  and  $c_s$  are the parameters of the so-called passive suspension;  $k_t$  stands for the tire stiffness; and  $M_s$  and  $m$  represent sprung (body) and unsprung (tire) masses, respectively. Moreover,  $x_s - x_u$  is the suspension stroke,  $x_u - x_0$  is the tire deflection, and  $x_0$  is the vertical ground displacement caused by road unevenness. The state variables of the model (4) are defined as  $x_1 = x_s - x_u$ ,  $x_2 = \dot{x}_s$ ,  $x_3 = x_u - x_0$ , and  $x_4 = \dot{x}_u$ . The disturbance due to the road roughness is  $\omega = \dot{x}_0$ . The normalized active force,  $u = u_f / u_s$ , is the control input, and  $u_f$  is the active force generated by a hydraulic actuator.

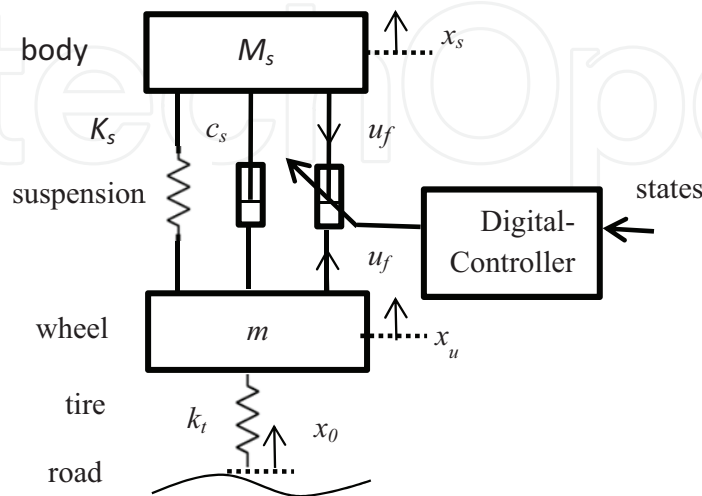


**Figure 1.** Quarter-car model with an active suspension.

The suspension performance, such as ride comfort, suspension deflection, and road holding, are considered as the control design objectives. Since the ride comfort can be quantified by the body acceleration in the vertical direction, it is reasonable to choose body acceleration as the regulated output,  $z(t)$ . The less the vertical body acceleration, the more comfort ride results [9]. One of the main objectives of the proposed controller is to minimize the vertical acceleration  $z(t)$  to improve vehicle ride comfort. The body acceleration is given by [9]

$$z = Cx + B_1 u \quad (6)$$

where

$$C = \frac{1}{M_s} [-k_s \quad -c_s \quad 0 \quad c_s], B_1 = \frac{u_s}{M_s} \quad (7)$$

In addition, due to the mechanical structure, the suspension stroke should not exceed the allowable maximum. Or equivalently, the active control force provided for the active suspension system should be confined to a certain range. Due to actuator saturation, it is in addition assumed that the normalized active force is bounded as  $|u(t)| \leq 1$ , **Figure 2**. Therefore, the bound on the control input is  $u_{max} = 1$ , and the active force is bounded by  $u_s$ .

Since microprocessors are widely used in car industries, system (4) can be discretized to design a discrete-time controller. Considering the disturbance effect later, the resulting discrete-time uncertain system with saturated control input is

$$x_{k+1} = (A + \Delta A_k)x_k + (B + \Delta B_k).sat(u_k) \quad (8)$$

where  $x_k$  and  $u_k$  are the state and control vectors of dimension  $n$  and  $m$ , respectively. The pair  $(A, B)$  is assumed to be controllable. The matrices  $\Delta A_k$  and  $\Delta B_k$  are time varying which represents parametric uncertainty due to changes in passenger load and/or nonlinearities. The uncertainty is assumed to be of the norm-bounded form:

$$[\Delta A_k, \Delta B_k] = M\Delta_k[N, N_b] \quad (9)$$

$$\Delta_k' \Delta_k \leq I \leftrightarrow \|\Delta_k\| \leq 1 \quad (10)$$

where  $M$  and  $N$  are known constant matrices with appropriate dimensions.  $\Delta_k$  is an unknown matrix with Lebesgue measurable elements.

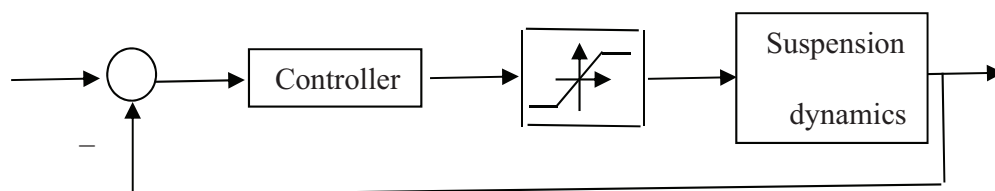


**Figure 2.** Feedback-saturated control systems.

The control signal is constrained due to practical limitation. The saturated controller to develop is assumed to be state feedback and symmetric and normalized as follows:

$$u = Fx, \quad -1 < u_j < +1, \quad j = 1 \dots m$$

or

$$\text{sat}(u_j) = \begin{cases} 1 & \text{if } u_j \geq 1 \\ u_j & \text{if } -1 < u_j < 1 \\ -1 & \text{if } u_j \leq -1 \end{cases} \quad (11)$$

$$u_k = Fx_k \quad (12)$$

The closed-loop system is given by

$$x_{k+1} = \{A + \Delta A_k + (B + \Delta B_k)F\}x_k \quad (13)$$

The problem is to develop a saturated discrete-time controller, which robustly stabilizes the closed-loop system (13) and ensures a good dynamic performance, described by maximum settling time and minimum damping ratio despite the system uncertainty. To achieve both constraints of max settling time and min damping ratio, the closed-loop poles must lie in the hatched area, as shown in **Figure 3**. This is termed D-stability in which the poles must lie inside

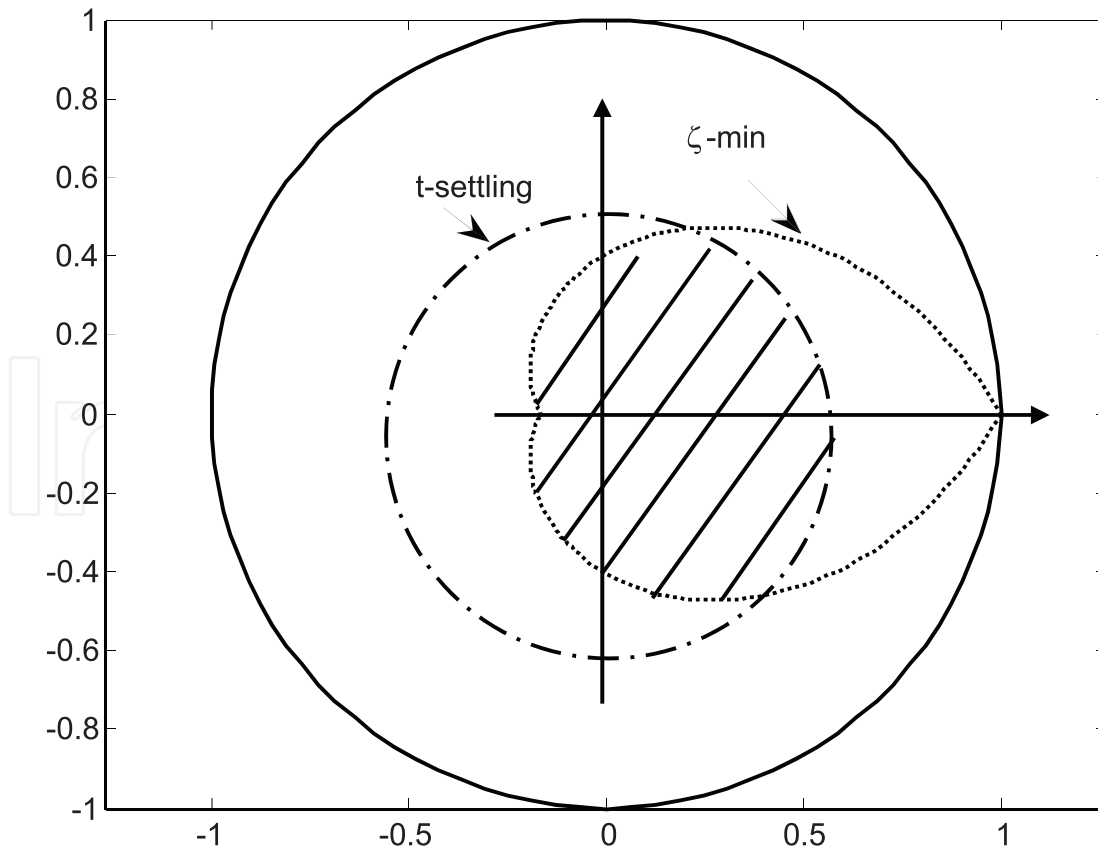


**Figure 3.** Desired region of closed-loop poles, hatched.

the region  $D$  for all admissible uncertainties. The proposed controller must achieve  $D$ -stability in addition to the constraint of maximum actuator control force.

### 3. Digital saturated regional pole placer

To design the abovementioned controller, the nonlinear saturated control function is first linearized and approximated by a convex hull. For this, the following two lemmas are used [21]:

#### Lemma-1

For all  $u \in \mathbb{R}^m$  and  $\theta \in \mathbb{R}^m$  such that  $|\theta_j| < 1, j \in [1, m]$ ,

$$\text{sat}(u) \in \text{co} \{ D_i u + D_i^- \theta, i \in [1, \eta] \}, \quad (14)$$

with  $\text{co}$  denoting the convex hull.

Eq. (14) has the following equivalent form:

$$\text{sat}(u) = \sum_{i=1}^{\eta} \gamma_i [D_i u + D_i^- \theta], \gamma_i \geq 0 \quad (15)$$

Here,  $D_i$  is an  $m \times m$  diagonal matrix with elements either 1 or 0 and  $D_i^- = (I - D_i)$ , which results in  $\eta = 2^m$  possible matrices. The matrices  $D_i$  and  $D_i^-$  are introduced to model the saturation function as a linear one. If  $D_i$  is selected as  $I$ ,  $D_i^-$  becomes 0, and the resulting controller will be unsaturated. Recall that these controllers (14) work in a linear region and do not allow saturation to occur.

The following sets are defined:

$$D(F) = \{ x \in \mathbb{R}^n : -1 \leq Fx \leq 1 \} \text{ and } \varepsilon(P, \rho) = \{ x \in \mathbb{R}^n : x^T P x \leq \rho; \rho > 0 \} \quad (16)$$

where  $P$  is a symmetric positive-definite matrix. The sets  $D(F)$  and  $\varepsilon(P, \rho)$  represent, respectively, a symmetrical polyhedral and an ellipsoidal one. The following result is recalled:

#### Lemma-2

For a given positive scalar  $\rho$ , if there exist matrices  $Y \in \mathbb{R}^{m \times n}$  and  $Z \in \mathbb{R}^{m \times n}$  and a positive-definite matrix  $X = X' \in \mathbb{R}^{n \times n}$  and solutions to the following LMIs:

$$[AX + B(D_i Y + D_i^- Z)] + \bullet < 0, \quad (17)$$

$$\begin{bmatrix} 1/\rho & Z_j \\ \bullet & X \end{bmatrix} > 0 \quad (18)$$

$$i = 1, \dots, \eta; j = 1, \dots, m, \quad (19)$$

then when  $\Delta A = 0$  and  $\Delta B = 0$ , the closed-loop saturated control system is asymptotically stable at the origin  $\forall x_0 \in \varepsilon(P, \rho)$  with

$$F = YX^{-1} \quad (20)$$

$$P = X^{-1} \quad (21)$$

It is worth mentioning that LMI (17) guarantees asymptotic stability, while LMI (17) ensures that the ellipsoidal set  $\varepsilon(P, \rho)$  is contained inside the polyhedral set  $D(H)$ , allowing the control to be saturated. As a special case, by selecting  $D_i = I$ , the control works only in a linear region without reaching saturation. In this case,  $D_i^- = 0$  in LMI (18), and  $Z_i$  is replaced by  $Y_i$  in LMI (17) to have  $\varepsilon(P, \rho) \subset D(F)$ .

Our control target is to design a saturated controller that maintains asymptotic stability against system uncertainty, as well as to place the closed-loop poles in a desired region D-stability, if possible, so as to achieve a good dynamic response in terms of settling time  $t_s$  and damping ratio  $\zeta$ .

Pole placement in the region shown in **Figure 3** is difficult to solve. However, the problem can be easily solved by approximating the spiral of the constant damping ratio as a circle, as shown in **Figure 4**. The problem is thus reduced to placing the poles in between the two circles, one for  $t_s$  and the other for  $\zeta_{approx}$ .

We will consider two design cases: without and with saturated inputs.

### Design case 1: unsaturated control

Consider the uncertain system with unsaturated control

$$x_{k+1} = (A + \Delta A)x_k + (B + \Delta B).u_k \quad (22)$$

### Theorem 1

If there is a feasible solution to the following LMIs, then the closed-loop poles lie inside the two circles of center  $q_1$  and radius  $r_1$  and center  $q_2$  and radius  $r_2$ :

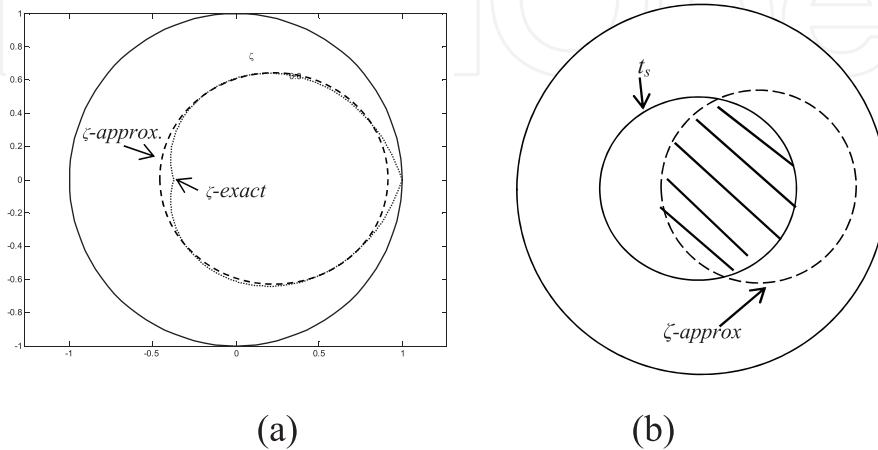


**Figure 4.** (a)  $\zeta$  circle approximation and (b) desired region of the poles, hatched.

$$X = X' > 0, \varepsilon_1 > 0, \varepsilon_2 > 0, v_1 > 0, v_2 > 0,$$

$$\begin{bmatrix} -r_1^2 X & \bullet & \bullet & \bullet \\ AX + BY + q_1 X & -X + (\varepsilon_1 + v_1)MM' & \bullet & \bullet \\ NX & 0 & -\varepsilon_1 I & \bullet \\ N_b X & 0 & 0 & -v_1 I \end{bmatrix} < 0 \quad (23)$$

$$\begin{bmatrix} -r_2^2 X & \bullet & \bullet & \bullet \\ AX + BY + q_2 X & -X + (\varepsilon_2 + v_2)MM' & \bullet & \bullet \\ NX & 0 & -\varepsilon_2 I & \bullet \\ N_b X & 0 & 0 & -v_2 I \end{bmatrix} < 0 \quad (24)$$

Moreover, the controller is given by

$$F = \Upsilon X^{-1} \quad (25)$$

*Proof*

It is well known [17] that the eigenvalues of matrix  $A$  lie inside a circle of center  $-q$  and radius  $r$  if and only if

$$P = P' > 0, \begin{bmatrix} -r^2 P & \bullet \\ A + qI & -P^{-1} \end{bmatrix} < 0 \quad (26)$$

or equivalently,

$$P = P' > 0,$$

$$\begin{bmatrix} -r^2 P & \bullet \\ A + BF + qI & -P^{-1} \end{bmatrix} + \left( \begin{bmatrix} 0 \\ M \end{bmatrix} \Delta(t) \begin{bmatrix} N' \\ 0 \end{bmatrix}' + \bullet \right) + \left( \begin{bmatrix} 0 \\ M \end{bmatrix} \Delta(t) \begin{bmatrix} F' N'_b \\ 0 \end{bmatrix}' + \bullet \right) < 0 \quad (27)$$

The last matrix inequality is satisfied if

$$P = P' > 0,$$

$$\begin{bmatrix} -r^2 P & \bullet \\ A + BF + qI & -P^{-1} \end{bmatrix} + \left( \varepsilon \begin{bmatrix} 0 \\ M \end{bmatrix} \begin{bmatrix} 0 \\ M \end{bmatrix}' + \varepsilon^{-1} \begin{bmatrix} N' \\ 0 \end{bmatrix} \begin{bmatrix} N' \\ 0 \end{bmatrix}' \right) \\ + \left( v \begin{bmatrix} 0 \\ M \end{bmatrix} \begin{bmatrix} 0 \\ M \end{bmatrix}' + v^{-1} \begin{bmatrix} F' N'_b \\ 0 \end{bmatrix} \begin{bmatrix} F' N'_b \\ 0 \end{bmatrix}' \right) < 0$$

is satisfied or

$$\begin{bmatrix} -r^2 P & \bullet & \bullet & \bullet \\ A + BF + qI & -P^{-1} + (\varepsilon + v)MM' & \bullet & \bullet \\ N & 0 & -\varepsilon I & \bullet \\ N_b F & 0 & 0 & -vI \end{bmatrix} < 0 \quad (28)$$

The last matrix inequality can be linearized by pre- and postmultiplying by  $[P^{-1}, I, I, I]$ , that is, applying fact 1 and substituting  $P^{-1} = X$ ,  $FX = Y$ .

Note that the above condition is only a sufficient condition for regional pole placement in one circle. Since we have to achieve pole placement in the area between the two circles, one for  $t_s$  and the other for  $\zeta$ , we have theorem 1.

### Design case 2: saturated control

Consider the uncertain system with saturated control

$$x_{k+1} = (A + \Delta A)x_k + (B + \Delta B).sat(u_k) \quad (29)$$

### Theorem 2

The regional pole placement with robust saturated state-feedback control (12) for the uncertain system (8) can be achieved if there exist  $X=X' > 0$ ,  $\varepsilon_1 > 0$ ,  $\varepsilon_2 > 0$ ,  $\nu_1 > 0$ ,  $\nu_2 > 0$ ,  $Y$  and a feasible solution to the following LMIs:

$$\begin{bmatrix} -r_1^2 X & \bullet & \bullet & \bullet \\ AX + B(D_i Y + \bar{D}_i Z) + q_1 X & -X + (\varepsilon_1 + \nu_1)MM' & \bullet & \bullet \\ NX & 0 & -\varepsilon_1 I & \bullet \\ N_b(D_i Y + \bar{D}_i HX) & 0 & 0 & -\nu_1 I \end{bmatrix} < 0 \quad (30)$$

$$\begin{bmatrix} -r_2^2 X & \bullet & \bullet & \bullet \\ AX + B(D_i Y + \bar{D}_i Z) + q_2 X & -X + (\varepsilon_2 + \nu_2)MM' & \bullet & \bullet \\ NX & 0 & -\varepsilon_2 I & \bullet \\ N_b(D_i Y + \bar{D}_i HX) & 0 & 0 & -\nu_2 I \end{bmatrix} < 0 \quad (31)$$

$$\begin{bmatrix} 1/\rho & Z_j \\ \bullet & X \end{bmatrix} > 0 \quad (32)$$

for  $i = 1, \dots, \eta$ ;  $j = 1, \dots, m$ .

Moreover, the saturated robust pole placer is given by

$$F = YX^{-1} \quad (33)$$

*Proof*

From (26), the poles of the closed-loop uncertain system (13) lie inside the circle of center  $(-q, 0)$  and radius  $r$  if and only if there is a feasible solution to the following LMI:

$$P = P' > 0$$

$$\begin{bmatrix} -r^2 P & \bullet \\ A + \Delta A + (B + \Delta B)(D_i F + \bar{D}_i^- H) + qI & -P^{-1} \end{bmatrix} < 0 \quad (34)$$

Eq. (34) is satisfied if the following inequality is satisfied:

$$P = P' > 0$$

$$\begin{bmatrix} -r^2 P & \bullet \\ A + B(D_i F + D_i^- H) + qI & -P^{-1} \end{bmatrix} + \varepsilon \begin{bmatrix} 0 \\ M \end{bmatrix} \begin{bmatrix} 0 \\ M \end{bmatrix}' + \varepsilon^{-1} \begin{bmatrix} N' \\ 0 \end{bmatrix} \begin{bmatrix} N & 0 \end{bmatrix} +$$

$$v \begin{bmatrix} 0 \\ M \end{bmatrix} \begin{bmatrix} 0 \\ M \end{bmatrix}' + v^{-1} \begin{bmatrix} (D_i F + \bar{D}_i H)' N_b' \\ 0 \end{bmatrix} \begin{bmatrix} N_b (D_i F + \bar{D}_i H) & 0 \end{bmatrix} < 0 \quad (35)$$

or equivalently,

$$\begin{bmatrix} -r^2 P & \bullet & \bullet & \bullet \\ A + B(D_i F + \bar{D}_i H) + qI & -P^{-1} + (\varepsilon + v)MM' & \bullet & \bullet \\ N & 0 & -\varepsilon I & \bullet \\ N_b (D_i F + \bar{D}_i H) & 0 & 0 & -vI \end{bmatrix} < 0 \quad (36)$$

By post- and premultiplying (36) by  $P^{-1}$ , that is, by applying the congruence transformation and substituting  $P^{-1} = X$ , one gets (30). This completes the proof.

#### 4. Design of vehicle active suspension control

In this section, we present a design example to illustrate the effectiveness of the proposed controller design method. Unlike the previous approaches, the proposed design introduces a digital computer or a microprocessor into the control loop as given in theorem 2. It is used to design an active suspension system for the quarter-vehicle model shown in **Figure 1** [9].

Note that active forces generated by hydraulic actuators and considered as control inputs are bounded because of actuator saturation. The system parameters and nominal values are shown in **Table 1**.

The normalized input is bounded as  $|u(t)| \leq 1$ , and the active force is bounded by  $u_s = \text{allowable spring stroke } (\pm 0.08 \text{ m}) \times \text{spring constant}$ .

Parameter	Value
$M_s$	320 kg
$m$	40 kg
$K_s$	18 kN/m
$k_t$	200 kN/m
$c_s$	1 kN.s/m
$u_s$	1.5 KN

**Table 1.** Quarter-vehicle active suspension parameters.

Due to different passenger load variations, it is assumed that the mass  $M_s$  varies between 250 to 390 kg. The system is discretized with the zero order hold method at a sampling time  $T_s=0.001$  sec. Therefore, the discrete time norm-bounded model is obtained as

$$A = \begin{bmatrix} 0.9997 & 0.000986 & 0.002476 & -0.0009852 \\ -0.05546 & 0.9969 & -0.007783 & 0.003106 \\ 0.0002228 & 1.245e-5 & 0.9975 & 0.0009867 \\ 0.4433 & 0.02485 & -4.934 & 0.9727 \end{bmatrix} \quad (37)$$

$$B = [2.089e-5 \quad 0.004622 \quad -1.857e-5 \quad -0.03694]' \quad (38)$$

With uncertainty matrices

$$M = [-0.0004 \quad -0.1367 \quad 0 \quad -0.0016]' \quad (39)$$

$$N = [-0.0729 \quad -0.0037 \quad -0.0102 \quad 0.0041], \quad (40)$$

$$N_b = 0.0061 \quad (41)$$

For passenger comfort, the oscillations due road bumps should be damped out within 1 s with a minimum damping ratio  $\zeta = 0.25$  [20]. To achieve the first objective, we select  $r_1 = 0.9960$  and  $q_1 = 0$  for the first circle, while for the second,  $r_2 = 0.68$  and  $q_2 = -0.31$ .

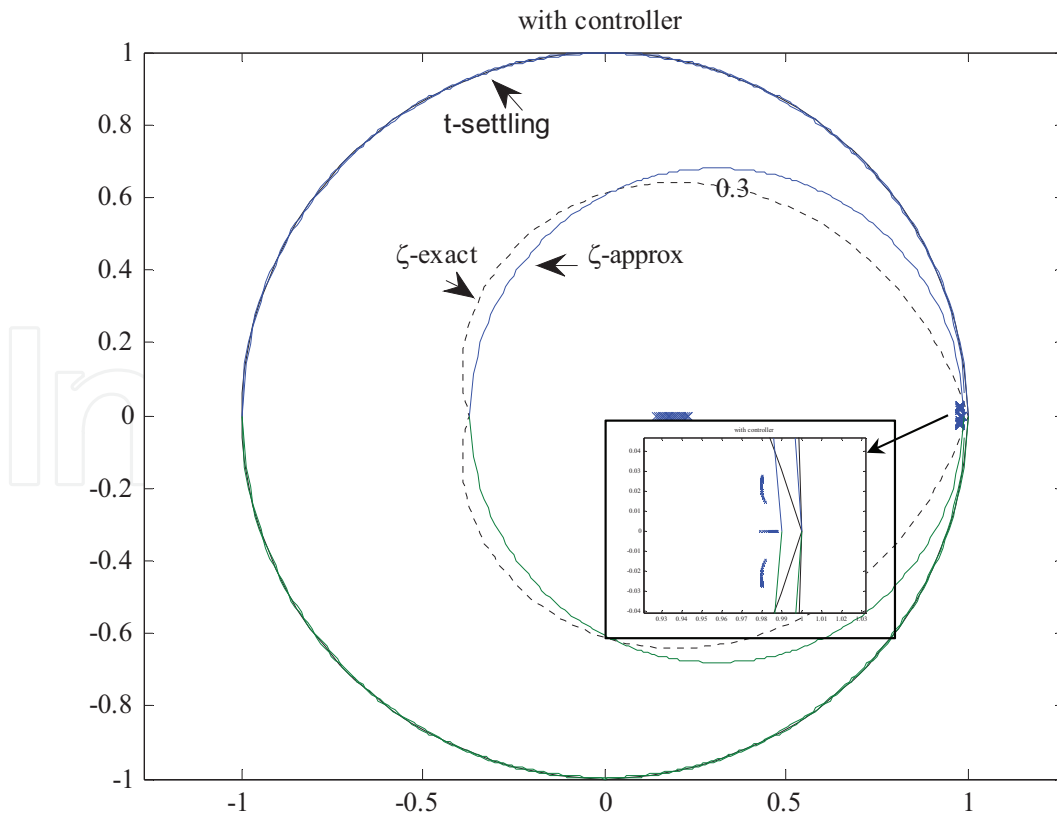


**Figure 5.** Closed-loop poles with system uncertainties using saturated control.

The LMIs (30) are solved to get the saturated control gain matrix as

$$F = [-402.7340, -47.9208, 546.4541, 16.1682] \quad (42)$$

As shown in **Figure 5**, all the closed-loop poles lie inside the desired domain.

In general, road disturbances can be classified as shock or vibration. For shock disturbances, the proposed controller is tested for two cases: step and bump road. The frequency response is studied when the system is subjected to resonant frequency disturbance forces for the vibration case.

### Case 1: step road test

For the simulation, we assume that the vehicle is subject to a 500 N unit step input due to a step road change. Two cases are considered: light and heavy passenger loads. With passive suspension, the vehicle will oscillate for an unacceptable long time, about 3.5 s, with large overshoot (**Figures 6 and 7**). This might damage the suspension system, whereas the active suspension damps the oscillations in about 0.3 s without overshoot (**Figures 6 and 7**).

### Case 2: road bump test

In order to study the system response due to road bump, the case of an isolated bump in an otherwise smooth road surface is considered [9]. The corresponding ground displacement in this case is given by

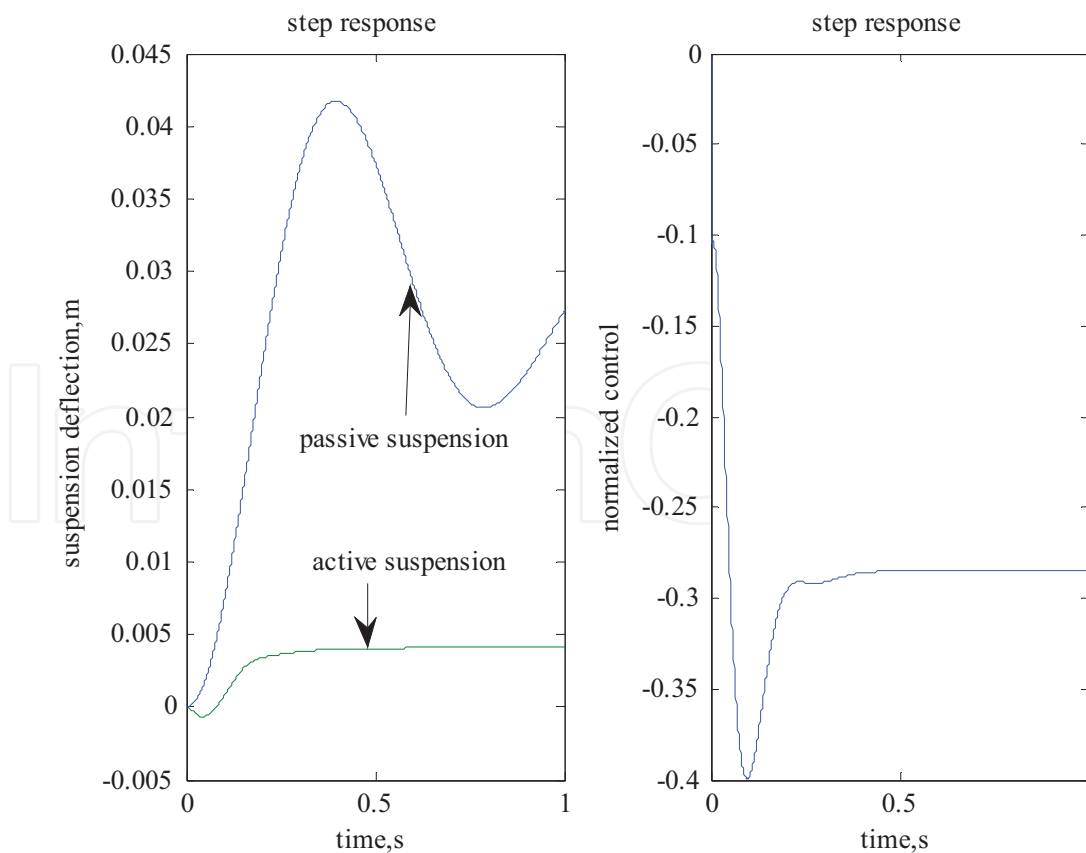


**Figure 6.** Step response at light load.

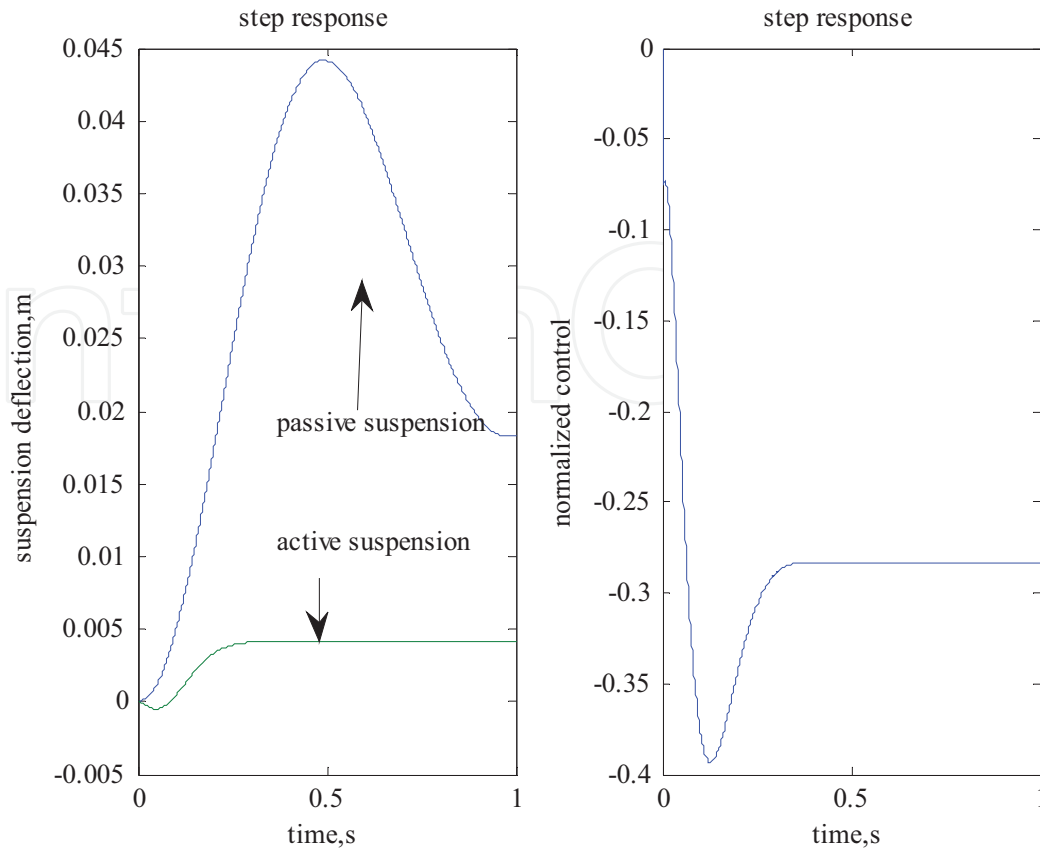


Figure 7. Step response at heavy load.

$$x_0 = \begin{cases} \frac{A}{2} \left[ 1 - \cos \left( \frac{2\pi V}{L} t \right) \right], & 0 \leq t \leq \frac{L}{V} \\ 0, & t > \frac{L}{V} \end{cases} \quad (43)$$

where  $A$  and  $L$  are the height and the length of the bump and  $V$  is the vehicle forward velocity. These values are chosen as  $A = 0.1$  m,  $L = 5$  m, and  $V = 27$  km/h. The bump response, namely, the suspension stroke (m) and the normalized control, is shown for two loads: light and heavy (**Figures 8 and 9**). In comparison with the passive suspension case, the proposed robust saturated control gives a better dynamic performance in terms of less overshoot and faster damping of the suspension stroke. Moreover, the normalized control signal is bounded between  $\pm 1$  as shown in **Figures 8 and 9**.

#### 4.1. Passenger comfort

The ride comfort is usually measured by the body acceleration as given in (6). This acceleration is shown in **Figure 10**.

It is evident from **Figures 6–10** that the active suspension outperforms the passive one since it satisfies the control objectives (damps out the oscillations in  $<1$  s and damping ratio  $> 0.25$ ) as

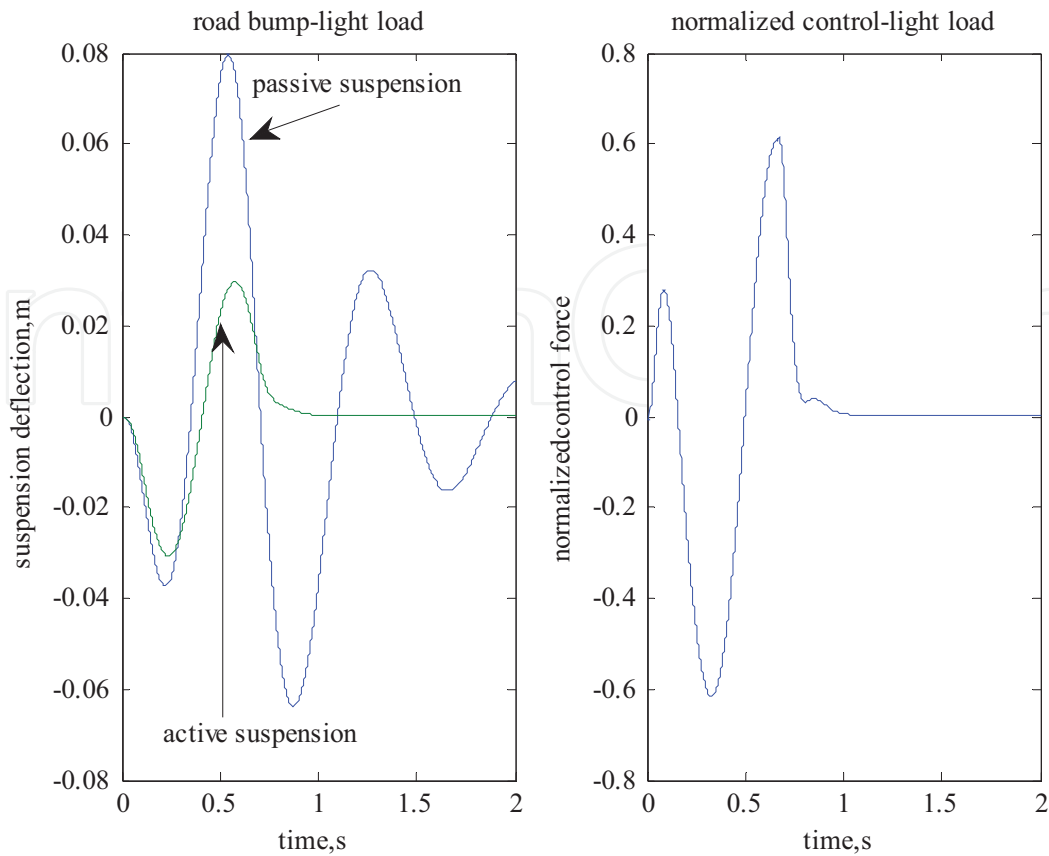


**Figure 8.** Road bump response at light load.

well as it does not violate the constraints of suspension stroke (8 cm) and hydraulic actuator force limit of 1.5 kN. Active suspension also provides better passenger comfort than the passive one as it has a lower body acceleration.

### Case 3: frequency response

It is well known that ride comfort is frequency sensitive. From the ISO2361, the human body is much sensitive to vertical vibrations in the frequency range of 4–8 Hz. Hence, further research work is needed to evaluate the designed constrained suspension in the frequency domain. In the analysis and design of linear systems, the relationship between the time domain and frequency domain characteristics plays an especially important role. However, in system design the state space in the time domain is more convenient as done in the proposed controller. In system analysis, conditions for the robust stability and robust performance are described as specifications on the frequency response in most cases. Therefore, it is indispensable to transform frequency domain conditions into equivalent time domain conditions in order to establish an effective design theory. Parseval's theorem gives the relationship between the squared integral of a time function and that of its Fourier transform, namely, the energy in the time domain is equal to the energy in the frequency domain. As a powerful tool bridging the time domain and frequency domain properties of systems, Kalman-Yakubovich-Popov (KYP) lemma plays a fundamental role in robust control.

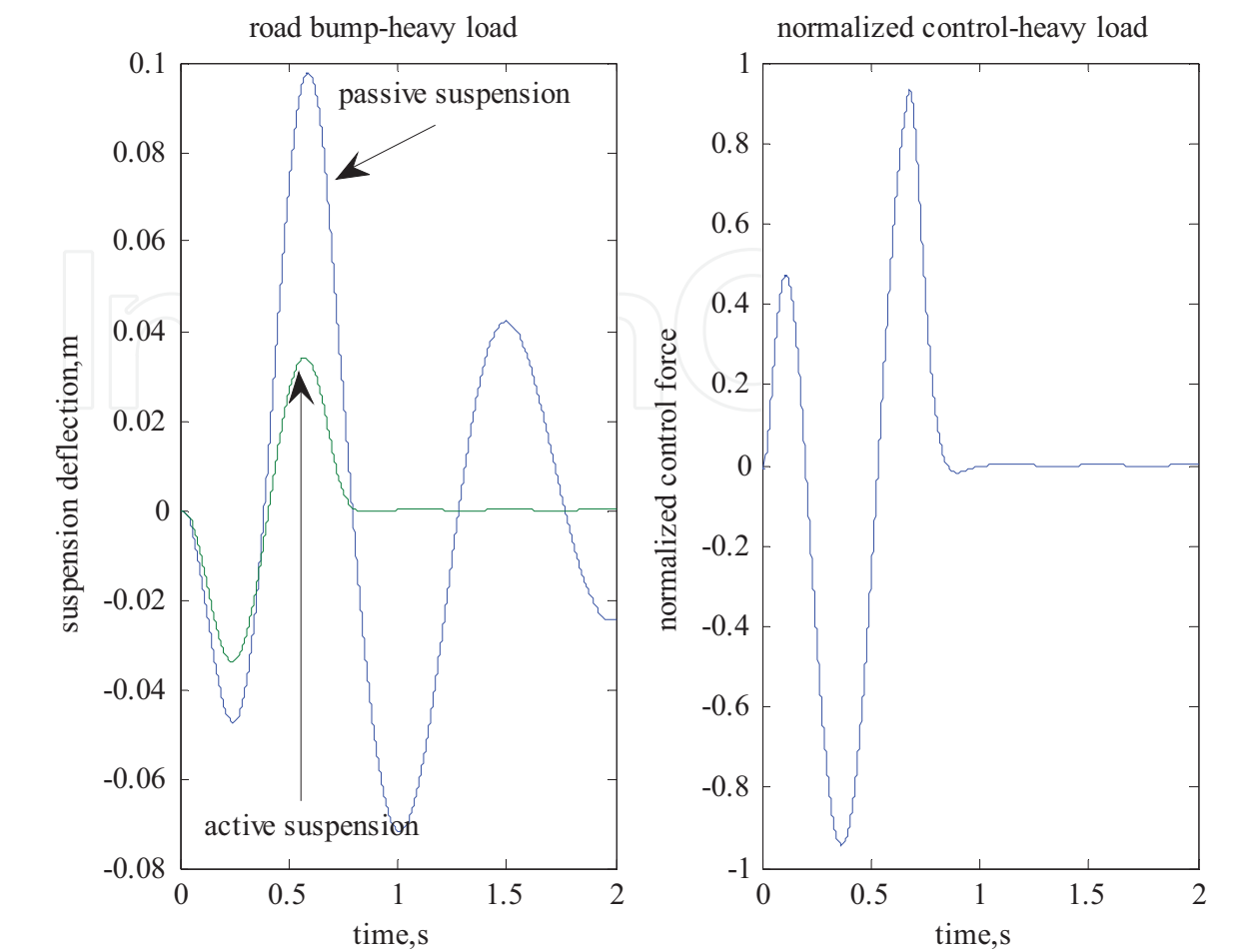


Figure 9. Road bump response at heavy load.

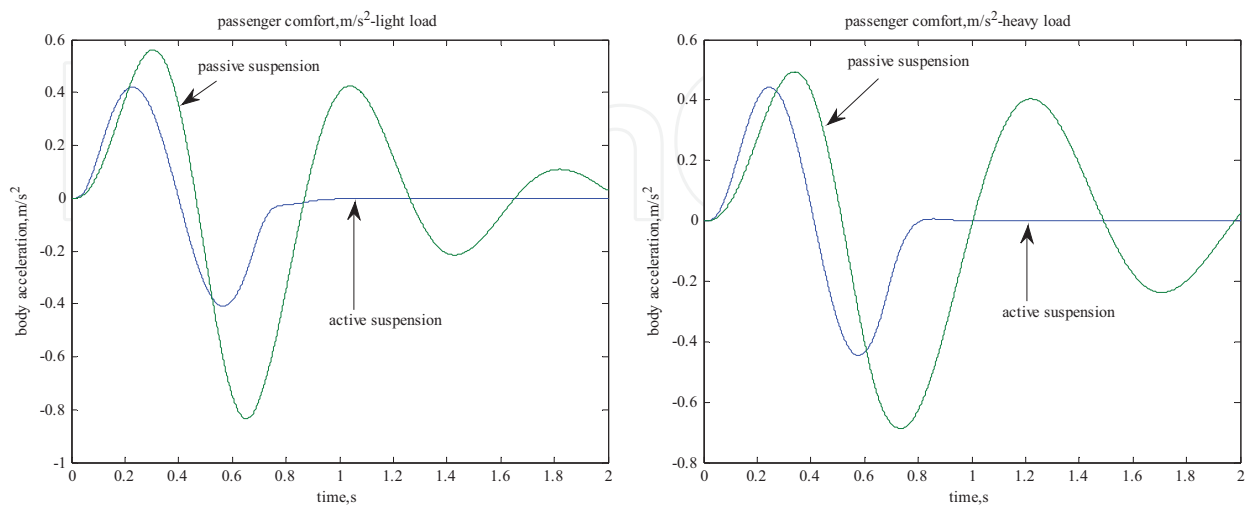


Figure 10. Passenger comfort due to road bump: light load (left) and heavy load (right).

## 5. Conclusion

This chapter considers placing the poles in a desired region of uncertain linear digital systems in the presence of input saturation. The new scheme is developed to design robust controllers, taking into consideration the effect of saturation nonlinearity. The proposed controller is based on LMI optimization and requires the uncertainty of model parameters to be cast in the norm-bounded form. The designed controller is applied to an active suspension of a quarter-vehicle model. Analysis and simulation results have confirmed the potential benefit of the proposed constrained active suspension in achieving the best possible ride comfort while keeping suspension strokes and control inputs within bounds.

In the future, it will be interesting to consider the actuator dynamic behavior in the controller design phase and also to develop robust control based on the relation between time domain and frequency domain properties.

## Author details

Hisham M. Soliman<sup>1,2\*</sup>, Rashid Al-Abri<sup>1</sup> and Mohammed Albadi<sup>1</sup>

\*Address all correspondence to: [hsoliman1@yahoo.com](mailto:hsoliman1@yahoo.com)

1 Department of Electrical and Computer Engineering, Sultan Qaboos University, Muscat, Oman

2 Electrical Engineering Department, Cairo University, Cairo, Egypt

## References

- [1] Cao D, Song X, Ahmadian M. Editors's perspectives: Road vehicle suspension design, dynamics, and control. *Vehicle System Dynamics*. 2011;**49**(1-2):3-28
- [2] Tseng HE, Hrovat D. State of the art survey: Active and semi-active suspension control. *Vehicle System Dynamics*. 2015;**53**(7):1034-1062
- [3] Fallah M, Bhat RB, Xie WF. Optimized control of semiactive suspension systems using H robust control theory and current signal estimation. *IEEE/ASME Transactions on Mechatronics*. 2012;**17**(4):767-778
- [4] Yagiz N, Hacıoglu Y. Backstepping control of a vehicle with active suspensions. *Control Engineering Practice*. 2008;**16**(12):1457-1467
- [5] Soliman HM, Awadallah MA, Nadim Emira M. Robust controller design for active suspensions using particle swarm optimization. *The International Journal of Modeling, Identification and Control*. 2008;**5**:66-76

- [6] Readman MC, Corless M, Villegas C, Shorten R. Adaptive Williams filters for active vehicle suspensions. *Transactions of the Institute of Measurement and Control*. 2010;**32**(6):660-676
- [7] Zuo L, Slotine JJ, Nayfeh SA. Model reaching adaptive control for vibration isolation. *IEEE Transactions on Control Systems*. 2005;**13**(4):611-617
- [8] Onat C, Kucukdemiral T, Sivrioglu S, Cansever YG. LPV gain scheduling controller design for a non-linear quarter-vehicle active suspension system. *Transactions of the Institute of Measurement and Control*. 2009;**31**(1):71-95
- [9] Chen H, Guo K. Constrained  $H^\infty$  control of active suspensions: An LMI approach. *IEEE Transactions on Control Systems Technology*. May 2005;**13**(3):412-421
- [10] Suzuki T, Takahashi M. Robust Active Suspension Control for Vibration Reduction of Passenger's Body. Chapter 5; *Challenges and Paradigms in Applied Robust Control* Edited by Andrzej Bartoszewicz. InTech; 2011. ISBN 978-953-307-338-5 472 p
- [11] Li H, Jing X, Karimi HR. Output-feedback-based  $H^\infty$  control for vehicle suspension systems with control delay. *IEEE Transactions on Industrial Electronics*. 2014;**61**(1):436-446
- [12] Li H, Jing X, Lam HK, Shi P. Fuzzy sampled-data control for uncertain vehicle suspension systems. *IEEE Transactions on Cybernetics*. 2014;**44**(7):1111-1126
- [13] Li H, Yu J, Hilton C, Liu H. Adaptive sliding-mode control for nonlinear active suspension vehicle systems using T-S fuzzy approach. *IEEE Transactions on Industrial Electronics*. August 2013;**60**(8)
- [14] Akbari A, Lohmann B. Output feedback HN/GH2 preview control of active vehicle suspensions: A comparison study of LQG preview. *Vehicle System Dynamics*. 2010;**48**(12):1475-1494
- [15] Mahmoud MS. *Decentralized Systems with Design Constraints*. London: Springer; 2011
- [16] Dorf R, Bishop RH. *Modern Control Systems*. 11th ed. New Jersey: Prentice Hall; 2008
- [17] Haddad WM, Bernstein DS. Controller design with regional pole constraints. *IEEE Transactions on Automatic Control*. 1992;**37**(1):54-69
- [18] Rao PS, Sen I. Robust pole placement stabilizer design using linear matrix inequalities. *IEEE Transactions on Power Systems*. Feb 2000;**15**:313-319
- [19] Mahmoud MS, Soliman HM. Design of robust power system stabilizer based on particle swarm optimization. *Circuits and Systems*. 2012;**3**:82-89
- [20] Soliman HM, Bajabaa N. Robust guaranteed-cost control with regional pole placement of active suspensions. *Journal of Vibration and Control*. June 2013;**19**(8):1170-1186
- [21] Benzaouia A. *Saturated Switching Systems*. Springer; 2012
- [22] Soliman HM, Benzaouia A, Yousef H. Saturated robust control with regional pole placement and application to car active suspension. *Journal of Vibration and Control*. 2016;**22**(1):258-269